

# Edge magnetoplasmon transport in gated and ungated quantum Hall systems

N. Kumada,<sup>1</sup> H. Kamata,<sup>1,2</sup> and T. Fujisawa<sup>2</sup>

<sup>1</sup>*NTT Basic Research Laboratories, NTT Corporation, 3-1 Morinosato-Wakamiya, Atsugi, Kanagawa 243-0198, Japan*

<sup>2</sup>*Department of Physics, Tokyo Institute of Technology, 2-12-1 Ookayama, Meguro, Tokyo 152-8551, Japan*

(Received 15 February 2011; revised manuscript received 6 May 2011; published 18 July 2011)

Edge magnetoplasmon (EMP) transport in gated and ungated quantum Hall systems is investigated by time-of-flight measurements. We measured the velocity, the amplitude, and the broadening of the EMP pulse injected by applying a voltage pulse to an Ohmic contact. We show that the transverse width of EMPs in the ungated sample is determined by the potential profile in the edge region, independent of the filling factor. In the gated sample, on the other hand, EMPs are confined by the innermost incompressible strip and their transverse width depends on the filling factor and the bulk electron density. We also find that scattering of EMPs by the bulk electrons is modified by the presence of the gate.

DOI: [10.1103/PhysRevB.84.045314](https://doi.org/10.1103/PhysRevB.84.045314)

PACS number(s): 73.43.-f, 73.20.Mf, 73.21.Fg

## I. INTRODUCTION

In a quantum Hall (QH) system, the Fermi energy lies between Landau levels and charged excitations have a gap in the interior of the two-dimensional electron system (2DES). Near the physical edge of the sample, the Landau levels move up by the confining potential and cross the Fermi energy, leading to compressible edge channels with gapless excitations separated by incompressible strips.<sup>1</sup> Since the chiral current in the edge channels is immune to back scattering, edge channels can be exploited as a tool to demonstrate electronic analogs of quantum optics experiments.<sup>2,3</sup> Recently, decoherence<sup>4-9</sup> and energy relaxation<sup>10-13</sup> in edge channels have been extensively investigated. The coherence and energy relaxation length depends on various parameters including Landau level filling factor  $\nu$ , dc bias, interactions between edge channels and with their environment, and the edge-state velocity.

The structure and charge velocity in edge channels can be measured through the transport of collective plasma oscillations called edge magnetoplasmons (EMPs).<sup>14</sup> EMPs have been investigated both theoretically<sup>14-16</sup> and experimentally.<sup>17-24</sup> Ashoori *et al.* performed time-of-flight measurements using an ungated sample with the edge defined by chemical etching and showed that the velocity of EMPs increases linearly with the Hall conductance  $\sigma_{xy}$ .<sup>19</sup> On the other hand, Zhitenev *et al.* showed that, in a sample covered with a gate, the velocity is smaller because of the screening of the electric field in EMPs and oscillates as a function of  $\nu$ .<sup>21</sup> The oscillation of the velocity has been explained by the oscillations of the width of the edge channels. Furthermore, recently, the velocity control at the fixed filling factor  $\nu = 2$  was demonstrated by changing the degree of screening by a gate.<sup>24</sup> These results suggest that the presence of a gate strongly affects the EMP transport. However, a systematic study of the gate effects on the EMP transport over a wide range of  $\nu$  is still lacking.

In this work, we carried out detailed time-of-flight measurements in samples with and without a front gate processed from the same wafer. This enables us to evaluate effects of the gate precisely. We injected EMPs in a pulse form and measured the velocity, the amplitude, and the broadening of the EMP pulse. The observed  $\nu$  dependence of the velocity is consistent with previous work:<sup>19,21</sup> in the ungated sample, the velocity

is proportional to  $\nu$ , while in the gated sample it oscillates with  $\nu$ . This clearly demonstrates that just the presence of the gate strongly alters EMP properties. An analysis of the results indicates that, in the ungated sample, the transverse width of EMPs is determined by the potential profile in the edge region almost independently of  $\nu$ . In the gated sample, on the other hand, EMPs are confined by the innermost incompressible strip and their width oscillates over 1 order of magnitude with  $\nu$ . At fixed  $\nu$ , the width increases with decreasing bulk 2DES density, reflecting the density dependence of the potential profile in the edge region. From the  $\nu$  dependence of the amplitude and the broadening of the EMP pulse, we find that scattering of EMPs by the bulk 2DES is also modified by the gate: EMPs are hardly scattered in the ungated sample, while the scattering rate oscillates with  $\nu$  in the gated sample.

This paper is organized as follows. Section II describes the sample structure, the experimental setup, and results of the dc measurement. In Secs. III A and III B, we present results of the time-of-flight measurement in the ungated and gated samples, respectively. In Sec. IV, we analyze the data and discuss EMP properties in both samples. The potential profile in the edge state is also discussed.

## II. EXPERIMENTAL SETUP AND DC MEASUREMENT

We used gated and ungated GaAs/Al<sub>0.3</sub>Ga<sub>0.7</sub>As samples. The 2DES is formed in a 20-nm-wide GaAs quantum well located  $d = 160$  nm below the surface. The low-temperature mobility is  $2.1 \times 10^6$  cm<sup>2</sup>/V s at an as-grown density of the 2DES  $n_0 = 1.2 \times 10^{11}$  cm<sup>-2</sup>. A schematic view of the sample structure and experimental setup is shown in the inset of Fig. 1. In the ungated sample, the sample edge is defined by chemical etching. In the gated sample, a Ti/Au (20/180 nm) front gate was deposited between the source S and drain D1 contacts after the chemical etching. The thickness of the gate metal is comparable to the etching depth and thus the side of the mesa is also covered with the metal. A quantum point contact (QPC) was fabricated close to the D1 contact. For the time-of-flight measurement, the QPC is set close to the pinch-off condition by applying a negative bias to the split gates. EMPs are injected by applying a square voltage pulse to the S contact; the width of the pulse is 5 ns and the amplitude is set at 5 mV within the linear conductance regime.<sup>22,25</sup> To detect EMPs, another

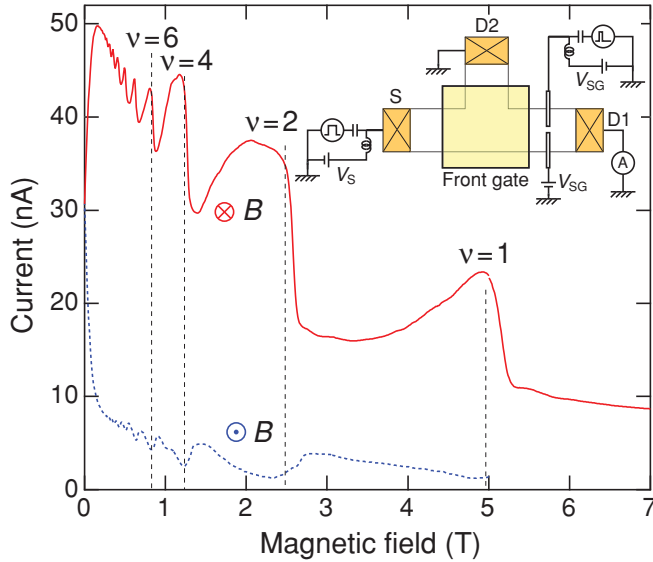


FIG. 1. (Color online) Results of the dc measurement for the ungated sample. A constant bias of 1.0 mV is applied to the S contact and the current through the D1 contact is plotted as a function of  $B$ . The split gate bias is set at 0 V. For the solid and dotted traces,  $B$  is applied from the front and back of the sample, respectively. Vertical dotted lines represent  $B$  for integer filling factors. The inset shows a schematic illustration (not to scale) of the sample structure and the experimental setup for the time-of-flight measurement.

voltage pulse with 1 ns in width and 100 mV in amplitude is superimposed on the dc bias for one of the split gates, by which the conductance of the QPC is temporally controlled. If the EMPs arrive at the QPC while it is open, they are transmitted through the QPC and detected as a current through the D1 contact; otherwise, they are reflected by the split gates and collected by the other drain contact D2. By controlling the time interval  $t$  between the injection and detection pulses, a profile of the EMP pulse is obtained.<sup>24</sup> The typical rise time of the pulses is 20 ps at the output of the pulse generator and is degraded to 50 ps at the sample; in the sample, the rise time is further degraded by various mechanisms including high Ohmic resistance and nonlinear dispersion of EMPs. The repetition time is 60 ns. All measurements were performed at 1.5 K.

The chirality of the edge current is examined by a three-terminal dc measurement. Figure 1 shows the current through the D1 contact in the ungated sample as a function of the magnetic field  $B$ . A constant bias of 1 mV is applied to the S contact. When  $B$  is applied from the front of the sample, the chirality is counterclockwise and the current takes peaks in the QH effect regime. On the other hand, when  $B$  is in the opposite direction, the chirality is clockwise and the current takes minima in the QH effect regime. Similar  $B$  dependence of the current was observed in the gated sample. For the time-of-flight measurements, the chirality is fixed to be counterclockwise, so that EMPs injected from the S contact propagate along the lower boundary to the QPC. In the ungated sample, the length of the edge channel between the S contact and the QPC is 1625  $\mu\text{m}$ . In the gated sample, the lengths in the regions with and without the front gate are 480 and 937  $\mu\text{m}$ , respectively.

### III. RESULTS OF TIME-OF-FLIGHT MEASUREMENT

#### A. Ungated sample

We first present results for the ungated sample. The color-scale plot in Fig. 2(a) is obtained by measuring the current through the D1 contact while sweeping  $t$  for each  $B$ . The  $t$  independent background is subtracted. Since the exact pulse delay caused by the cables is unknown, we here define  $t = 0$  as the time at the onset of the current at  $B = 0$  T; at  $B = 0$  T the injected electrons propagate as two-dimensional plasmons, which have a velocity much higher than that of EMPs (Ref. 14) and thus propagate without detectable delay.

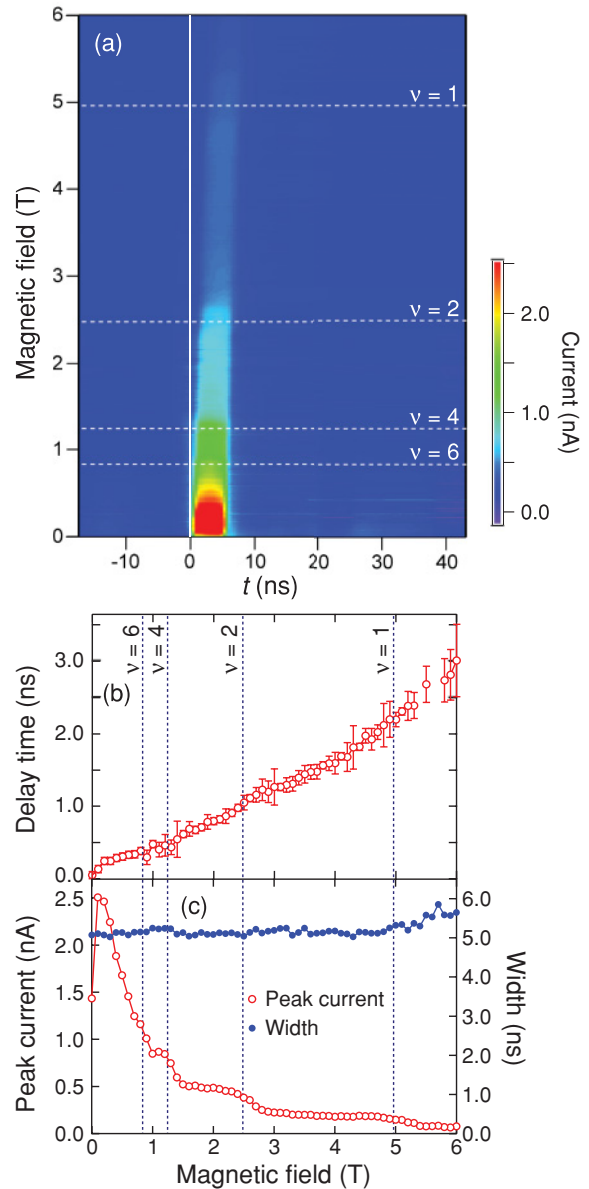


FIG. 2. (Color online) Results of the time-of-flight measurement for the ungated sample. (a) Current through the D1 contact is plotted as a function of the time interval  $t$  between the injection and detection pulses and  $B$ . The solid vertical line represents  $t = 0$ . Dashed horizontal lines represent  $B$  for the integer filling factors. (b) Delay time; (c) the peak current and the full width at half maximum of the EMP pulse as a function of  $B$ .

In the magnetic field, EMPs appear as the current pulse with a time delay. Note that we observed only a single EMP mode; acoustic EMP modes with nodes in the electron density in the transverse direction<sup>15,26</sup> would be damped during the long-distance (1625  $\mu\text{m}$ ) propagation.

In Figs. 2(b) and 2(c), the delay time, the peak current, and the full width at half maximum of the EMP pulse are plotted as a function of  $B$ . The delay time increases almost linearly with  $B$ , consistent with previous work using ungated samples.<sup>19,26</sup> The peak current decreases with steps at integer  $\nu$ . Note that the absolute value of the peak current has little meaning because it is changed by the condition of the QPC

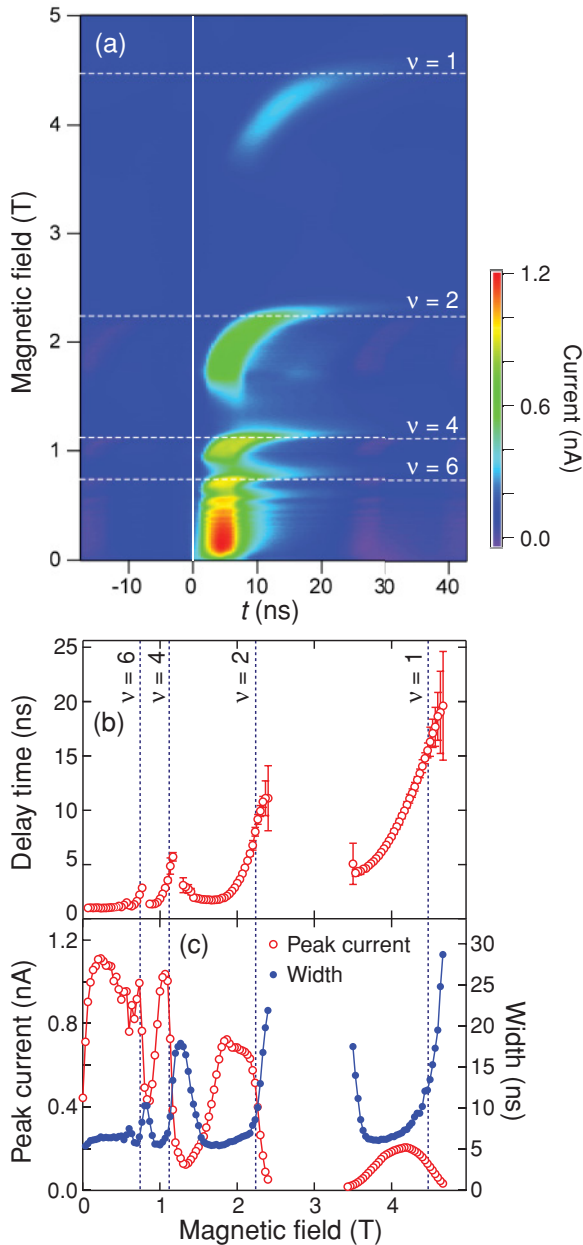


FIG. 3. (Color online) Results of the time-of-flight measurement for the gated sample for  $V_f = 0$  V. (a) Current through the D1 contact is plotted as a function of  $t$  and  $B$ . (b) Delay time; (c) the peak current and the full width at half maximum of the EMP pulse as a function of  $B$ .

detection. The width of the EMP pulse is as small as that of the injection pulse (5 ns) over the whole experimental range.

### B. Gated sample

Figure 3 presents results for the gated sample. The front gate bias is fixed at  $V_f = 0$  V. The density in the gated region is  $n_0 = 1.08 \times 10^{11} \text{ cm}^{-2}$ . The data clearly demonstrate that the transport properties of EMPs are strongly altered by the presence of the front gate. The delay time generally increases with  $B$  and asymmetric oscillations with maxima at integer  $\nu$  are superimposed on the trend [Fig. 3(b)], consistent with previous work using gated samples.<sup>21,23</sup> Furthermore, the peak current and the width of the EMP pulse also oscillate as a function of  $B$  [Fig. 3(c)]. For  $B \lesssim 0.5$  T, the pulse is slightly broader than that in the ungated sample because of the presence of the parallel capacitance between EMPs or two-dimensional plasmons and the front gate. As  $B$  is increased across  $B$  for an integer  $\nu$ , the EMP pulse becomes low and broad abruptly. In particular, for  $3.4 > B > 2.4$  T and  $B > 4.7$  T, the pulse width is larger than the repetition time (60 ns) and the current peak was not observed. Note that the  $B$  dependence of the peak current is similar to that of the dc current (Fig. 1).

## IV. ANALYSES AND DISCUSSION

In Fig. 4(a), the velocity of EMPs calculated from the delay time and the length of the edge channels is plotted as a function of  $\nu$ ; to obtain the velocity in the gated region, the contribution of the ungated region in the gated sample is subtracted by using the velocity in the ungated sample. The plot includes the velocity in the gated region for lower electron densities  $n_0 = 0.89$  and  $0.7 \times 10^{11} \text{ cm}^{-2}$  obtained by applying negative biases  $V_f = -0.05$  and  $-0.1$  V, respectively. In the ungated region, the velocity is on the order of 1000 km/s and increases linearly with  $\nu$ . In the gated region, the velocity is about 1 order of magnitude smaller and oscillates with  $\nu$ . At fixed  $\nu$ , the velocity decreases with decreasing  $n_0$ .

### A. Ungated sample

The velocity of EMPs has been theoretically investigated. In the ungated 2DES with the density profile,

$$n(x) = \frac{2n_0}{\pi} \arctan \sqrt{\frac{x}{a}}, \quad x \geq 0, \quad (1)$$

where  $x$  is the transverse coordinate, the velocity at a wave number  $k$  is given by<sup>14,15</sup>

$$v = \frac{d\omega(k)}{dk} = \frac{[\ln(e^{-\gamma}/2ka) - 1]\sigma_{xy}}{\epsilon}, \quad (2)$$

where  $\gamma$  is the Euler constant, and  $\epsilon$  is the dielectric constant. In this model, EMPs are localized within a strip of width  $a$ , where  $dn/dx$  is large. The observed linear  $\nu$  dependence of the velocity (Fig. 4) can be explained by the  $\nu$  dependence of  $\sigma_{xy}$ . As shown in the inset of Fig. 4(a), the experimental result is well reproduced by the fitting with  $ka = 8.1 \times 10^{-3} \pm 0.4 \times 10^{-3}$ ; for the fitting, we used the linear relation  $\sigma_{xy} = \nu e^2/h$  because plateaux in  $\sigma_{xy}$  are small at 1.5 K. Although  $k$  is not unique in the square pulse, if we assume the wave length to be the length of the edge (1625  $\mu\text{m}$ ),  $a$  is estimated to be

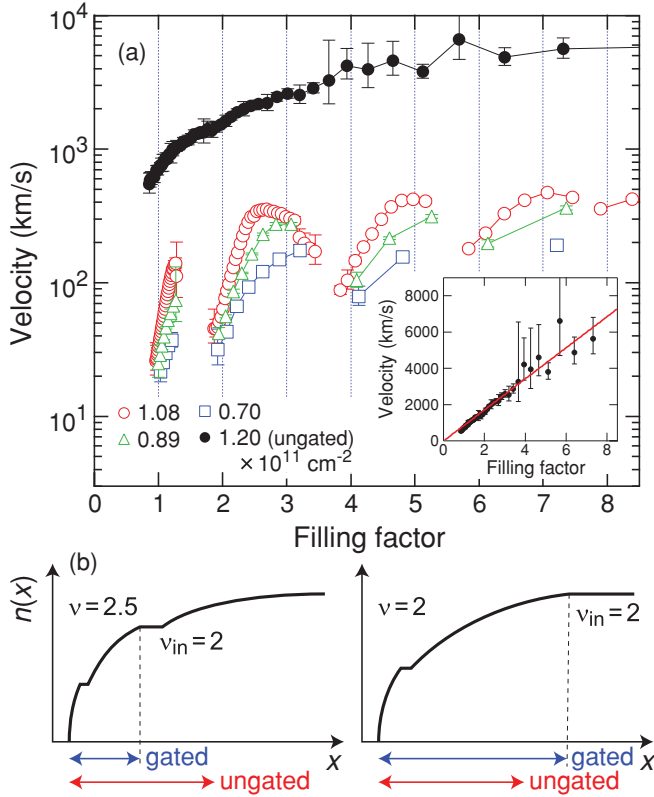


FIG. 4. (Color online) (a) Log-scale plot of the velocity of EMPs in the ungated (solid symbols) and gated (open symbols) regions as a function of  $\nu$ . Inset shows the linear-scale plot of the velocity in the ungated region. The line is the result of the fitting. (b) Illustration of the density profile  $n(x)$  in the edge state and the transverse extent of EMPs in the ungated and gated regions represented by arrows for the bulk filling factors  $\nu = 2.5$  and 2.

$\sim 2 \mu\text{m}$ .<sup>27</sup> This value is consistent with a typical width of the edge region.<sup>28</sup> The result that  $a$  is constant indicates that detailed edge structure does not lead to a large modification of EMPs. Although the EMP mode density should be zero in incompressible strips, where charged excitation has a gap, EMPs can extend across incompressible strips through long-range interactions<sup>16</sup> and  $a$  is simply determined by the potential profile at zero magnetic field as illustrated in Fig. 4(b).

The step-like behavior of the peak current and the sharp EMP pulse [Fig. 2(c)] indicate that EMPs are hardly scattered during the  $1625 \mu\text{m}$  propagation. This is consistent with a photovoltage measurement<sup>29</sup> for higher temperature ( $>4.2 \text{ K}$ ) and lower field ( $<2 \text{ T}$ ) range, which shows that the mean free path of EMPs is longer than  $900 \mu\text{m}$  around  $4.2 \text{ K}$ . However, this is not trivial because the dc current in the same sample oscillates with  $\nu$  (Fig. 1). In the dc transport, a scanning force microscopy<sup>28</sup> showed that the current is confined in edge channels when the incompressible strip separating edge channels and the bulk 2DES is wide, while the current is scattered and spreads to the whole bulk when the incompressible strip is narrow. Accordingly, the dc current oscillates with  $\nu$ , reflecting the width of the incompressible strip and the longitudinal conductance of the bulk 2DES. The change in the current distribution with the edge structure has been explained by a calculation for a stationary nonequilibrium

situation, in which local equilibrium was assumed.<sup>30</sup> We suggest that the difference between the EMP and dc transport comes from the short duration of the EMP pulse, which corresponds to the sum of the time width of the injection pulse (5 ns) and the traveling time of EMPs ( $<3 \text{ ns}$ ): for the EMP transport, the duration is shorter than the scattering time, where the local equilibrium condition is not satisfied, and then EMPs can arrive at the detection QPC without scattering. It is worth noting that, since EMPs spread across incompressible strips [Fig. 4(b)], scattering mechanism for electrons in dc transport and high-frequency EMPs would be different. For further understanding of the scattering mechanism, experiments in a sample with longer edge and thus longer traveling time are necessary.

### B. Gated sample

In the gated 2DES, long-range interactions across incompressible strips are screened and EMPs are confined by an incompressible strip when the distance  $d$  between the gate and the 2DES is smaller than the width of the incompressible strip. According to Refs. 21 and 31,  $d = 160 \text{ nm}$  in our sample is larger than the width of outer incompressible strips, while can be smaller than that of the innermost incompressible strip. As a result, EMPs are expected to be confined by the innermost incompressible strip and then transverse width of EMPs in the gated sample  $w$  becomes qualitatively different from that in the ungated sample  $a$ . The gate also screens the in-plane electric field in EMPs, by which the velocity of EMPs is reduced. For  $d \ll w$ , the degree of the screening is evaluated by  $d/w$  and the velocity is given by<sup>16,22</sup>

$$v = \frac{\sigma_{xy}d}{\epsilon w}. \quad (3)$$

The observed smaller velocity in the gated region is due to the screening of EMPs. For the  $\nu$  dependence of the velocity,  $\sigma_{xy}$  only explains its increasing tendency; therefore, the oscillations of the velocity are ascribed to the  $\nu$  dependence of  $w$ . In addition, the change in the velocity with  $n_0$  at fixed  $\nu$  indicates that  $w$  depends also on  $n_0$ .

In Fig. 5(a),  $w$  calculated by using Eq. (3) with  $\sigma_{xy}$  of the innermost incompressible strip is plotted as a function of  $\nu$ .  $w$  oscillates between  $\sim 0.3$  and  $\sim 3 \mu\text{m}$  and takes maxima at integer  $\nu$ . The oscillations of  $w$  as a function of  $\nu$  have been explained by the oscillations of the position of the incompressible strip.<sup>21</sup> To explain the scenario, we start from the case of  $\nu = 2.5$ , where the filling factor of the innermost incompressible strip is  $\nu_{\text{in}} = 2$  [Fig. 4(b)]. As the bulk filling factor is decreased to  $\nu = 2$ , the  $\nu_{\text{in}} = 2$  incompressible strip moves toward the interior of the 2DES and, hence,  $w$  increases. As  $\nu$  is decreased below 2, the  $\nu_{\text{in}} = 2$  incompressible strip vanishes and then the  $\nu_{\text{in}} = 1$  incompressible strip becomes the boundary between the edge and the bulk, resulting in an abrupt decrease in  $w$ . The same argument applies for larger  $\nu$ , reproducing the asymmetric oscillations of  $w$  with respect to integer  $\nu$ .

The oscillation of the EMP velocity and of the position of the incompressible strip contributes to the oscillations of the peak current and the width of the EMP pulse [Fig. 3(c)]. As an example, we consider the behavior for  $4 > \nu \geq 2$ . For

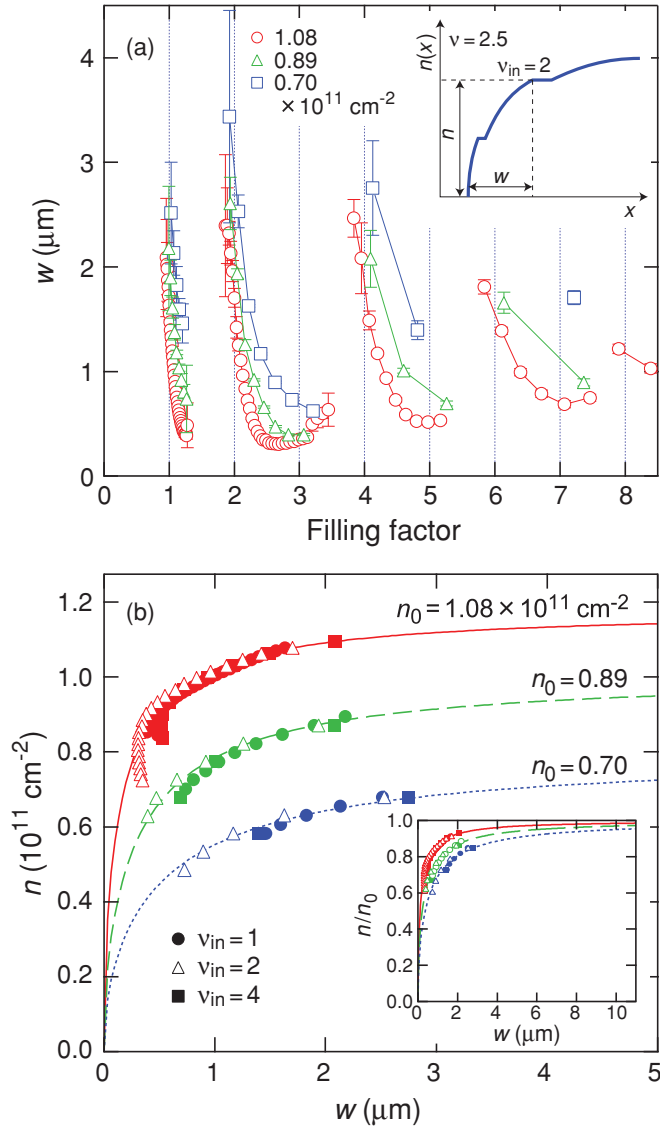


FIG. 5. (Color online) (a) Transverse width of EMPs in the gated region calculated by using Eq. (2) as a function of  $\nu$ . Inset shows an illustration of the density profile in the edge region for the bulk filling factor  $\nu = 2.5$ . (b) Electron density of the innermost incompressible strip  $n = n_0 \nu_{\text{in}} / \nu$  is plotted as a function of  $w$  for the three values of  $n_0$ . Circles, triangles, and squares are the results obtained when the innermost incompressible strip is  $\nu_{\text{in}} = 1, 2,$  and  $4$ , respectively. Lines are results of the fitting. The inset shows the normalized density  $n/n_0$  as a function of  $w$ .

$\nu$  slightly smaller than 4, the  $\nu = 2$  incompressible strip is close to the mesa edge, at which the edge potential is steep and the incompressible strip is narrow. In this case, EMPs are easily scattered by the bulk 2DES as discussed for the dc transport<sup>28,30</sup> and the EMP pulse becomes broad and small. As  $\nu$  is decreased to  $\sim 3$ , the incompressible strip moves away from the mesa edge and thus becomes wide, leading to the sharp EMP pulse with large amplitude. On further decreasing  $\nu$  to 2, although the incompressible strip continues to be wider, the traveling time of EMPs increases and the damping of the EMP pulse during the travel slightly increases. Note that also at the boundary between the gated and ungated regions,

where EMP properties changes discontinuously, EMPs would be scattered.

The  $n_0$  dependence of  $w$  can be explained by the change in the edge potential. Since we know the density  $n = n_0 \nu_{\text{in}} / \nu$  of the innermost incompressible strip at a position  $w$  [inset of Fig. 5(a)], the density profile in the edge potential is obtained by compiling the dataset  $(w, n)$ .<sup>23</sup> Figure 5(b) shows  $n$  as a function of  $w$  for the three values of  $n_0$ . Data for the filling factor range with the innermost incompressible strip  $\nu_{\text{in}} = 1, 2,$  and  $4$  are plotted in different symbols. They follow a single curve, indicating that the position of the incompressible strip is determined by the electrostatic force and that the many-body physics in the edge state does not affect  $w$ , at least within our experimental resolution. Note that, for  $n_0 = 1.08 \times 10^{11} \text{ cm}^{-2}$ , the data for  $\nu_{\text{in}} = 2$  and  $4$  deviate from the curve when  $w$  is small, which is probably due to the appearance of weak  $\nu = 3$  and  $5$  QH states. The normalized density  $n/n_0$  as a function of  $w$  is plotted in the inset of Fig. 5(b). The plot shows that the slope of the edge potential is gentler for smaller  $n_0$ . The density profiles are phenomenologically reproduced by the form  $n(w) = n_0 [w / (w + 2l)]^{1/2}$  with the depletion length  $l = 0.17, 0.33,$  and  $0.55 \mu\text{m}$  for  $n_0 = 1.08, 0.89,$  and  $0.7 \times 10^{11} \text{ cm}^{-2}$ , respectively. It should be noted that since the theory<sup>1,32</sup> for the fitting function is based on the model for a gate defined edge without a gate on top of the 2DES, which is different from our experimental condition, the quantitative value of  $l$  obtained by the fitting has little meaning. Nevertheless, the qualitative change in  $l$  provides an intuitive interpretation for the  $n_0$  dependence of  $w$ . Namely, the increase in  $l$  with decreasing  $n_0$  implies that, as  $n_0$  is decreased, the overall edge state moves into the interior of the sample, where the potential slope is gentler, leading to larger  $w$ .

## V. CONCLUSIONS

In conclusion, we carried out systematic time-of-flight measurements of edge magnetoplasmons in ungated and gated samples. In the ungated sample, the transverse width of EMPs is determined by the profile of the edge potential, independent of  $\nu$ . EMPs are hardly scattered by the bulk 2DES during the  $1625 \mu\text{m}$  propagation. In the gated sample, on the other hand, EMPs are confined by the innermost incompressible strip. The width oscillates as a function of  $\nu$ , following the oscillation of the position of the incompressible strip. The scattering rate of EMPs also oscillates, reflecting the velocity of EMPs and the width of the incompressible strip. These results demonstrate that the presence of the gate strongly modifies the transport properties in QH edge channels. We also showed that the edge potential becomes gentler as the electron density in the bulk 2DES decreases. This explains the density dependence of the width of EMPs.

## ACKNOWLEDGMENTS

The authors are grateful to K. Muraki, T. Ota, and M. Hashisaka for fruitful discussions and to M. Ueki for experimental support. This work was supported in part by Grant-in-Aid for Scientific Research (21000004) from MEXT of Japan.

- <sup>1</sup>D. B. Chklovskii, B. I. Shklovskii, and L. I. Glazman, *Phys. Rev. B* **46**, 4026 (1992).
- <sup>2</sup>Y. Ji, Y. Chung, D. Sprinzak, M. Heiblum, D. Mahalu, and H. Shtrikman, *Nature (London)* **422**, 415 (2003).
- <sup>3</sup>I. Neder, N. Ofek, Y. Chung, M. Heiblum, D. Mahalu, and V. Umansky, *Nature (London)* **448**, 333 (2007).
- <sup>4</sup>L. V. Litvin, H.-P. Tranitz, W. Wegscheider, and C. Strunk, *Phys. Rev. B* **75**, 033315 (2007).
- <sup>5</sup>P. Roulleau, F. Portier, D. C. Glatli, P. Roche, A. Cavanna, G. Faini, U. Gennser, and D. Mailly, *Phys. Rev. Lett.* **100**, 126802 (2008).
- <sup>6</sup>L. V. Litvin, A. Helzel, H.-P. Tranitz, W. Wegscheider, and C. Strunk, *Phys. Rev. B* **78**, 075303 (2008).
- <sup>7</sup>I. P. Levkivskiy and E. V. Sukhorukov, *Phys. Rev. B* **78**, 045322 (2008).
- <sup>8</sup>S. C. Youn, H. W. Lee, and H. S. Sim, *Phys. Rev. Lett.* **100**, 196807 (2008).
- <sup>9</sup>D. T. McClure, Y. Zhang, B. Rosenow, E. M. Levenson-Falk, C. M. Marcus, L. N. Pfeiffer, and K. W. West, *Phys. Rev. Lett.* **103**, 206806 (2009).
- <sup>10</sup>C. Altimiras, H. le Sueur, U. Gennser, A. Cavanna, D. Mailly, and F. Pierre, *Nat. Phys.* **6**, 34 (2010).
- <sup>11</sup>H. le Sueur, C. Altimiras, U. Gennser, A. Cavanna, D. Mailly, and F. Pierre, *Phys. Rev. Lett.* **105**, 056803 (2010).
- <sup>12</sup>C. Altimiras, H. le Sueur, U. Gennser, A. Cavanna, D. Mailly, and F. Pierre, *Phys. Rev. Lett.* **105**, 226804 (2010).
- <sup>13</sup>P. Degiovanni, Ch. Grenier, G. Féve, C. Altimiras, H. le Sueur, and F. Pierre, *Phys. Rev. B* **81**, 121302 (2010).
- <sup>14</sup>V. A. Volkov and S. A. Mikhailov, *Zh. Eksp. Teor. Fiz.* **94**, 217 (1988) [*Sov. Phys. JETP* **67**, 1639 (1988)].
- <sup>15</sup>I. L. Aleiner and L. I. Glazman, *Phys. Rev. Lett.* **72**, 2935 (1994).
- <sup>16</sup>M. D. Johnson and G. Vignale, *Phys. Rev. B* **67**, 205332 (2003).
- <sup>17</sup>D. C. Glatli, E. Y. Andrei, G. Deville, J. Poitrenaud, and F. I. B. Williams, *Phys. Rev. Lett.* **54**, 1710 (1985).
- <sup>18</sup>V. A. Volkov, D. V. Galshenkov, L. A. Galchenkov, I. M. Grodnenskii, O. R. Matov, and S. A. Mikhailov, *Pis'ma Zh. Eksp. Teor. Fiz.* **44**, 510 (1986) [*JETP Lett.* **44**, 665 (1986)].
- <sup>19</sup>R. C. Ashoori, H. L. Stormer, L. N. Pfeiffer, K. W. Baldwin, and K. West, *Phys. Rev. B* **45**, 3894 (1992).
- <sup>20</sup>V. I. Talyanskii, A. V. Polisski, D. D. Arnone, M. Pepper, C. G. Smith, D. A. Ritchie, J. E. Frost, and G. A. C. Jones, *Phys. Rev. B* **46**, 12427 (1992).
- <sup>21</sup>N. B. Zhitenev, R. J. Haug, K. v. Klitzing, and K. Eberl, *Phys. Rev. B* **49**, 7809 (1994).
- <sup>22</sup>N. B. Zhitenev, R. J. Haug, K. V. Klitzing, and K. Eberl, *Phys. Rev. B* **52**, 11277 (1995).
- <sup>23</sup>G. Ernst, N. B. Zhitenev, R. J. Haug, and K. von Klitzing, *Phys. Rev. Lett.* **79**, 3748 (1997).
- <sup>24</sup>H. Kamata, T. Ota, K. Muraki, and T. Fujisawa, *Phys. Rev. B* **81**, 085329 (2010).
- <sup>25</sup>We confirmed that the EMP signal is linear at least down to 0.5 mV.
- <sup>26</sup>G. Ernst, R. J. Haug, J. Kuhl, K. von Klitzing, and K. Eberl, *Phys. Rev. Lett.* **77**, 4245 (1996).
- <sup>27</sup>Since, for the observed velocity range, the length of the EMP pulse with the duration of 5 ns is longer than the length of the edge, we used  $k = 2\pi/(1.625 \times 10^{-6})$  to estimate  $a$ .
- <sup>28</sup>E. Ahlswede, P. Weitz, J. Weis, K. von Klitzing, and K. Eberl, *Physica B* **298**, 562 (2001).
- <sup>29</sup>V. M. Muravev, I. V. Kukushkin, A. L. Parakhonskii, J. Smet, and K. von Klitzing, *JETP Lett.* **83**, 246 (2006).
- <sup>30</sup>K. Güven and R. R. Gerhardt, *Phys. Rev. B* **67**, 115327 (2003).
- <sup>31</sup>G. Sukhodub, F. Hohls, and R. J. Haug, *Phys. Rev. Lett.* **93**, 196801 (2004).
- <sup>32</sup>K. Lier and R. R. Gerhardt, *Phys. Rev. B* **50**, 7757 (1994).